Interaction of Room Temperature Ionic Liquid Solutions with a Cholesterol Bilayer

S. R. T. Cromie, M. G. Del Pópolo, and P. Ballone*

Atomistic Simulation Centre, Queen's University Belfast, Belfast BT7 1NN, U.K.

Received: May 1, 2009; Revised Manuscript Received: June 16, 2009

Water solutions of representative ([C_4mim][Cl] and [C_4mim][Tf_2N]) room temperature ionic liquids (ILs) in contact with a neutral lipid bilayer made of cholesterol molecules has been investigated by molecular dynamics simulations based on an empirical force field model. The results show that both ILs display selective adsorption at the water−cholesterol interface, with partial inclusion of ions into the bilayer. In the case of [C_4mim][Cl], the adsorption of ions at the water−cholesterol interface is limited by a sizable bulk solubility of the IL, driven by the high water affinity of $[Cl]^-$. The relatively low solubility of [C_4mim][Tf_2N], instead, gives rise to a nearly complete segregation of the IL component on the bilayer, altering its volume, compressibility, and electrostatic environment. The computational results display important similarities to the results of recent experimental measurements for ILs in contact with phospholipid model membranes (see Evans, K. O. *Int. J. Mol. Sci.* **2008**, *9*, 498−511 and references therein).

I. Introduction

The release of new chemical species in the environment always requires an extensive stage of monitoring and testing for their biological effects, especially when the new compounds are characterized by unusual bonding and chemical properties. In this respect, a case in point is represented by room temperature ionic liquids (ILs),[1] that is, organic ionic compounds whose melting temperature is below 373 K, that are currently considered for a wide range of applications in the so-called *green* version of industrial processes.[2]

Even though, in most cases, the usage of ILs appears to be relatively safe and potentially beneficial for the environment, their biological effects are still partly unknown.[3] Recent experiments,[4−6] for instance, have revealed strong association of ILs with phospholipid membranes, leading at high concentration to the disruption of the phospholipid bilayer, especially in the case of ILs with long hydrocarbon side chains. To be sure, the IL concentrations considered in the chemical physics experiments of refs 4−6 are orders of magnitude higher than those expected to arise in biological tissue from environmental pollution. Nevertheless, the experimental observations point to aspects that need a closer scrutiny, especially taking into account that the complexity of living organisms, together with the intricate interdependence of biochemical pathways, almost guarantees that unexpected effects are the most likely result of introducing new chemicals into our environment. On the other hand, strong and specific interaction with membranes of ionic and, in some cases, amphiphilic compounds such as ILs might have fundamental implications for pharmacology applications or biomedical technologies concerning, in particular, novel strategies to deliver drugs to cells across their protective membrane.[8−10]

We investigate the microscopic details of IL/membrane interactions by performing a molecular dynamics simulation of two prototypical ILs ([C_4mim][Cl] and [C_4mim][Tf_2N]; see the schematic structure in Figure 1) of the alkyl-imidazolium family dissolved in water and in contact with a model membrane made of a cholesterol bilayer. The choice of cholesterol has been dictated in part by the fairly small size of this amphiphilic molecule, somewhat limiting the cost of the computation. Moreover, we recently performed an extensive investigation of cholesterol/water systems, showing that the computational models provide a fair account of the properties of cholesterol clusters[11] and compact layers[12] deposited *on* water or solvated *in* water. Finally, the neutral character of cholesterol implies that the simulation results represent a kind of lower bound for the membrane interaction with ionic species. On the other hand, the dominant interaction mechanisms might be different in cholesterol and in phospholipids that, at variance from cholesterol, tend to be ionic or zwitterionic at near physiological conditions, and the comparison with experimental results still requires considerable caution.

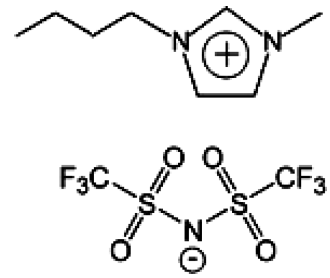

Figure 1. Schematic structure of $[C_4mim]^+$ (top) and $[Tf_2N]^-$ (bottom).

In our computations, we consider IL concentrations comparable to those used in the experiments and much higher than those expected to be relevant for environmental safety. A series of simulations for cholesterol bilayers in contact with NaCl and LiCl water solutions have been performed to provide a comparison for the IL case.

Despite the obvious differences between the lipids considered in experiments (phospholipids) and in our simulations (cholesterol), the two sets of results display several close analogies, suggesting that the interplay of hydrophilic/hydrophobic character in lipids and in ILs represents the primary reason for their close association to bilayers. In the case of [C_4mim][Cl], in particular, we observe a partial penetration of the butyl tail of

* Corresponding author. E-mail: p.ballone@qub.ac.uk.

10.1021/jp904060y CCC: $40.75
Published on Web 08/05/2009

$[C_4mim]^+$ into the cholesterol bilayer, limited by the tendency of $[Cl]^-$ to remain solvated in water. In the case of $[C_4mim][Tf_2N]$, instead, we observe nearly complete segregation of the IL at the water−cholesterol interface. The $[Tf_2N]^-$ anion is partially incorporated into the bilayer, causing a limited penetration of the positively charged imidazolium ring while, at the same time, decreasing the close adsorption of the butyl tail of $[C_4mim]^+$.

In contrast, the addition of [Li][Cl] or [Na][Cl] to the water environment surrounding the bilayer has only minor effects on its properties, both in experiments and in simulations.

II. The Experimental Picture

The effect of ILs of the alkyl-methyl-imidazolium family on the stability of large unilamellar vesicles made of phospholipids such as 1,2-dielaidoylphosphocholine (DEPC) and 1,2-dimyristoylphosphoglycerol (DMPG) recently has been the subject of comprehensive experimental investigations,[4−6] motivated mainly by biocatalysis applications. Measurements have been carried out using a combination of fluorescence spectroscopy,[4] dynamic light scattering,[4] quartz microbalance measurements,[5,6] and atomic force microscopy.[6] To isolate the effect of the individual ions, measurements have been performed on solutions containing either alkyl-imidazolium ($[C_nmim]^+$, $n = 4 - 8$) or $[Tf_2N]^-$, paired to simpler inorganic ions ($[Cl]^-$ for $[C_nmim]^+$ and $[Li]^+$ for $[Tf_2N]^-$).[7]

Fluorescence spectroscopy, in particular, was used in ref 4 to detect the leakage of fluorescent markers from vesicles, whereas dynamic light scattering was used to monitor the size of vesicles in equilibrium with different electrolyte solutions.

The results show that dissolving ILs into water always induces measurable leakage from vesicles. Moreover, the IL effect increases with increasing length of the alkyl chain and with the hydrophobicity of the anion. The leakage induced by $[C_4mim][Cl]$, for instance, is far from complete and takes place over a relatively long time (approximately 10 min). This, in turn, suggests that it is mediated by small, localized defects, possibly due to the insertion of $[C_4mim]^+$ into the DEPC bilayer. Leakage is nearly complete, meaning that almost every vesicle is leaking, already in the case of $[C_6mim][Cl]$. Moreover, leakage takes place very quickly, suggesting that it occurs by massive poration or by some other substantial disruption of the bilayer. Finally, most IL anions do not seem to interact strongly with the phospholipid bilayer, the exception being represented by hydrophobic anions such as $[Tf_2N]^-$, which at high concentration gives rise to extensive leakage, even when it is coupled to a simple cation such as $[Li]^+$. By contrast, solutions of simple electrolytes, such as [Na][Cl], have only a minor effect on the vesicles' integrity.

Further experiments have been reported in ref 5, focusing on the effect of ILs on the formation kinetics and stability of phospholipid bilayers deposited on solid surfaces made of silica, oxidized gold, and gold surfaces modified by an organic self-assembled monolayer. The results largely confirm the qualitative findings of ref 4, highlighting the strong interaction between the IL and the lipid bilayer, competing with and prevailing upon the bilayer−surface interactions. Finally, AFM measurements reported in ref 6 provide topographic information on the defects generated by ILs on lipid bilayers, showing that $[Tf_2N]^-$, in particular, gives rise to mesoscopic pores throughout the membrane.

III. The Model and the Simulation Method

We consider a system made of cholesterol, water, and electrolyte species, represented by $[C_4mim][Cl]$ and $[C_4mim][Tf_2N,]$. As a comparison, [Na][Cl] and [Li][Cl] solutions have been considered, as well.

Cholesterol is described by an Amber-type potential described in detail in ref 11. The actual model parameters are listed in the supporting information of that reference. The potential is tuned on the results of density functional computations for the molecular geometry, torsional energy, and hydrogen bonding of cholesterol and water, as well as on experimental data for the structure and equilibrium volume of two different phases of cholesterol[13] and one cholesterol monohydrate crystal form.[14]

Water is described by the flexible 3-center potential (SPC/Fw) introduced and validated in ref 15. The dispersion (van der Waals) cross-interaction of water and cholesterol deviates somewhat from ideal mixing as given by the Berthelot rule. As discussed in ref 11, the interaction of the water−oxygen with cholesterol carbons is reduced to 75% of the ideal mixing value, whereas the interaction of water−oxygen with cholesterol hydrogens is reduced to 80% of the ideal mixing value. This modification is required to ensure the stability of cholesterol islands and of dense overlayers on water.

The molecular interactions of the ILs $[C_4mim][Cl]$ and $[C_4mim][Tf_2N]$ have been modeled by the potential given in ref 16. In this case, ideal mixing has been used for the dispersion part of the cross-interactions of ILs with both water and cholesterol.[17] Simple electrolytes such as NaCl and LiCl are modeled by the Fumi−Tosi potential[18] using formal charges ($q_i = \pm e$). The cross-interactions for the dispersion part have been estimated by resorting to the Lennard-Jones parameters for the salt ions listed in ref 19, whose mixing properties with water have been thoroughly tested. We did not use this last form and parametrization for the direct interaction of alkali and halide ions because the Fumi−Tosi potential still represents one of the most accurate models for the pure phases, even though in this case, the difference might be relatively unimportant, since both LiCl and NaCl completely dissociate in water at the conditions of our simulation, and their ions interact mainly through Coulomb forces that are the same in both models.

Periodic boundary conditions are used, and long-range Coulomb interactions are accounted for using Ewald sums.

Simulations have been carried out using the DL_POLY package[20] running on parallel clusters. The size of the simulation cell has been adjusted during a first equilibration run of 1 ns in the NPT ensemble and then kept fixed in a second equilibration stage of 3 ns. We verified that structural and energy contributions fluctuated in time without apparent drift beyond the equilibration stage. The length of the production runs is specified below for the different systems. Simulations covering 1 ns typically required 2.5 days on 12 nodes of an itanium cluster.

IV. Results

All simulations started from a well-equilibrated sample consisting of a cholesterol bilayer in water (see Figure 2). The model membrane, in turn, was made of 80 cholesterol molecules arranged on two layers, spanning an area of 40.5×38 Å^2. The water side of the interface is represented by 2850 H_2O molecules, and the system is enclosed in a nearly orthorhombic simulation cell whose base is parallel to the bilayer and with a height of 90 Å. The system volume has been relaxed by molecular dynamics in the NPT ensemble, followed by further equilibration and a sequence of production runs in the NVT ensemble. The results of these simulations, reported in ref 12, show that the bilayer is liquidlike and the cholesterol molecule displays a sizable mobility, with a diffusion constant $D = 18 \pm 2 \times 10^{-7}$ cm^2/s. Statistical analysis of the bilayer fluctuations[21]

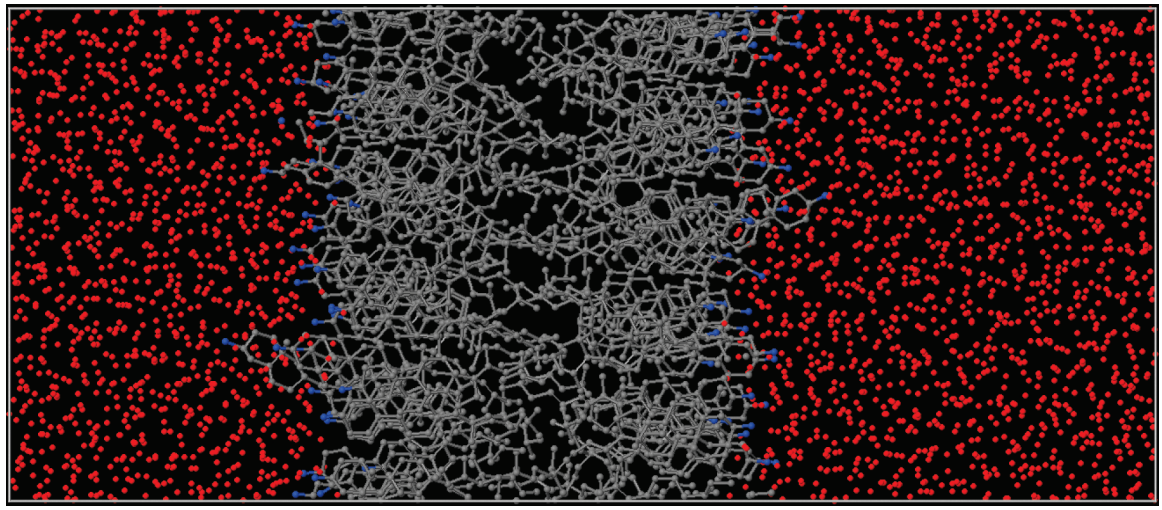

Figure 2. Cholesterol bilayer in water. Black particles, carbon; red, water oxygen; blue, cholesterol oxygen. Hydrogen not shown.

shows that the interfacial tension with water vanishes within the estimated error bar, while bending rigidity remains as the leading elastic response of the bilayer. Moreover, we observe that, even on average, the bilayer deviates somewhat from planar, since the interaction with water gives rise to a small-amplitude but still apparent stationary wave commensurate with the simulation box. The coincidence of the modulation wavelength with the simulation box side is obviously an artifact of periodic boundary conditions, and no experimental data is available to verify whether a comparable corrugation is present in real cholesterol bilayers in water. The modulation of the average position, however, is relatively small, with an amplitude of 4 Å over a 40.5 Å wavelength, and as shown in Figure (2), the interface of cholesterol with pure water is always well-defined and certainly stable over the time scale of our simulations.

The addition of the electrolyte is carried out by placing ions at random positions within the simulation box. Overlapping water molecules are removed, while insertion attempts giving rise to short contacts with membrane atoms are rejected. As a consequence of this initialization strategy, the simulated samples contain a slightly different number of water molecules that in all cases exceeds 2500. Moreover, the electrolyte is fully dissociated, and ions are distributed approximately uniformly in the volume occupied by water, and no ion is in close contact with the bilayer in the starting configuration.

For both [C_4mim][Cl] and [C_4mim][Tf_2N], 20 ion pairs have been added, resulting in a 0.37 M solution. As anticipated in Section III, the volume has been relaxed for 1 ns in the NPT ensemble, followed by an additional 3 ns equilibration. All simulations have been carried out at $T = 280$ K, and for the NPT runs, pressure is set to $P = 1$ atm. By monitoring the diagonal elements of the stress tensor, we verified that the system remains isotropic and that pressure is close to 1 atm also during the NVT runs.

Samples evolve quickly and systematically in the early stages of equilibration, which is favored by the fluid character of all components in the system and by the sizable forces associated to the random position of the ions. The drift of thermodynamic and structural quantities dies off within the first two nanoseconds of equilibration, and then the system settles into a near-equilibrium condition characterized by fluctuations without apparent drift. For each system, statistics have been collected over 10 ns. Relaxation processes taking place on time scales much longer than the simulation time are likely to be present, as suggested by the macroscopic times of the system evolution in the experiments. For obvious reasons, however, these processes cannot be detected by our statistical analysis.

Snapshots taken from the [C_4mim][Cl] and [C_4mim][Tf_2N] simulations are shown in Figure 3a and b. The difference between these two representative configurations is apparent.

In the case of [C_4mim][Cl], adsorption of ions at the bilayer coexists with a still sizable IL solubility in water, driven by the high solubility of $[Cl]^-$. In the case of [C_4mim][Tf_2N], the IL precipitates out of the solution, apparently because of the much lower affinity of $[Tf_2N]^-$ for water. Moreover, and more importantly for our discussion, this second IL gives rise to a nanometer thick deposit at the water/cholesterol interface. Residual solubility is observed in the form of very few ions dissolved in water. From time to time, we observe molecularly thin whiskers protruding from the IL film into the water and consisting of a chainlike arrangement of neutral cation−anion pairs. Previous studies have shown that in ILs, these structural motifs arise from the association of ions into neutral polar molecules[22] bound by dipolar forces into chainlike aggregates. In most cases, whiskers emerge and return to the IL film, thus giving rise to closed dipolar loops.

To verify the reproducibility of this picture, we repeated the [C_4mim][Tf_2N] simulation with a larger sample made of the same 80-molecule bilayer with, however, 30 ion pairs dissolved into ~4000 water molecules, corresponding to 0.38 M electrolyte concentration. The simulation box is again nearly orthorhombic, with volume $40.5 \times 38 \times 116$ Å^3. The preparation and the equilibration of the system are completely analogous to those of the smallest sample. In addition, the simulation results are similar, even though the kinetics of the system relaxation toward equilibrium is slightly more complex in the largest sample. In this case, the initial precipitation gives rise to a few distinct nanometric IL blobs floating in water that, by ripening, are progressively incorporated into the adsorbed film. This is a relatively slow process that is not completed on the time scale of our simulations. As a result, one IL aggregate consisting of a few ion pairs still floats in water 10 ns after the end of equilibration. However, the size of this residual isolated aggregate tends to decrease over time, although slowly and with some fluctuations, and we expect its eventual inclusion into the IL film adsorbed at the cholesterol interface. More importantly for our discussion, the close association of ions with the cholesterol membrane and the formation of a film between the

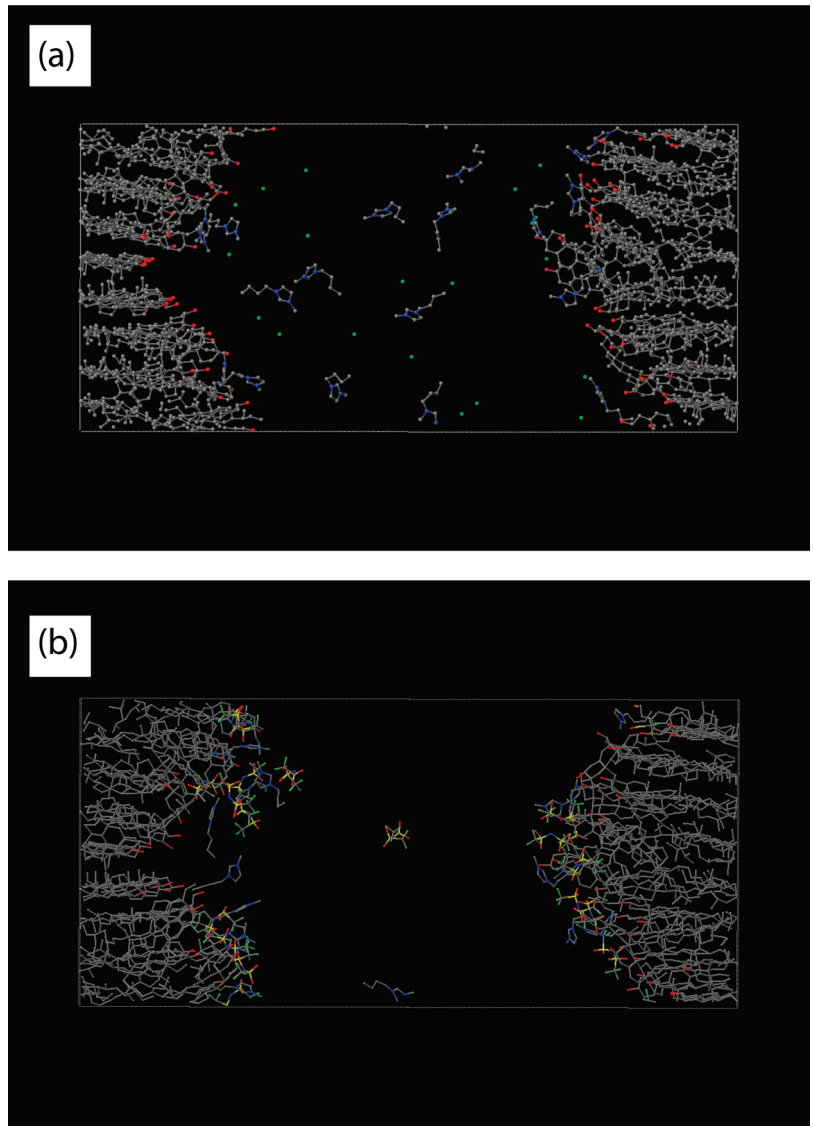

Figure 3. Simulation snapshot of a 0.37 M electrolyte solution in contact with a cholesterol bilayer: (a) [C_4mim][Cl], (b) [C_4mim][Tf_2N]. Black particles, carbon; red, oxygen; blue, nitrogen; dark green, chlorine (panel a) or fluorine (panel b); yellow, sulfur. Hydrogen not shown.

cholesterol and water is confirmed by this last simulation for the largest sample.

Detailed analysis of snapshots for both[C_4mim][Cl] and [C_4mim][Tf_2N] solutions reveals characteristic differences in the contact region of IL and cholesterol whose relations with the experimental data of ref 4 are discussed in the following section. In the case of [C_4mim][Cl], for instance, the closest approach to cholesterol is due to the butyl tail of the cation that becomes partially incorporated into the bilayer. In the case of [C_4mim][Tf_2N], instead, it is the bulky [Tf_2N]$^-$ anion that is directly in contact with cholesterol, displaying, also in this case, partial incorporation into the model membrane (see Figure 4).

Simulations for the same bilayer in contact with an electrolyte solution containing 50 NaCl or 50 LiCl ions pairs, corresponding to 0.9 M concentration, do not display any sizable association of the electrolyte with cholesterol. Both salts are fully dissociated, and ions remain well-solvated in water. Because of the lower complexity and the higher mobility of these electrolytes, production runs have been limited in this case to 2 ns.

To provide a more quantitative picture of the system evolution, we define and compute the density profile of water and ILs with respect to the cholesterol membrane. Since this last is not even approximatively planar and, in any case, its position fluctuates in time, we refer the distribution of water and ions to the instantaneous location of the bilayer boundary, defined as follows. For every configuration, the location of the bilayer at position (x_0, y_0) on the basal plane of the simulation box is found by moving a test particle of radius R_T along the straight line parallel to the z direction and going through the point (x_0, y_0, z). The upper boundary of the bilayer is identified with the height $z_U(x_0, y_0)$ at which the first contact with a non-hydrogen cholesterol atom takes place when moving the test particle from far above the bilayer. No periodic boundary conditions are applied along z at this stage. Moreover, contact is defined to take place when the separation of the test particle and the cholesterol atom is equal to the radius R_T of the external probe. In a similar way, the lower boundary of the bilayer is identified with the height $z_L(x_0, y_0)$ at which the test particle first touches a non-hydrogen cholesterol atom while approaching from far below the bilayer. The detailed result of this construction, of course, depends on the choice of R_T, but the picture emerging from our analysis is nearly the same, provided R_T is close to the size of an average atom. In what follows, the value $R_T = 3.5$ Å as been adopted.

The two surfaces $z_U(x, y)$ and $z_L(x, y)$ are conceptually analogous to the intrinsic surface defined in ref 23 for the case

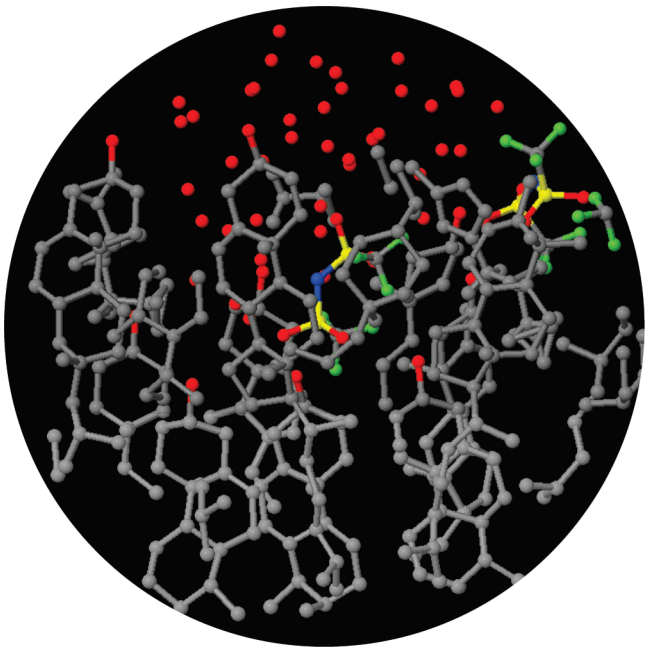

Figure 4. Snapshot view of the local cholesterol arrangement around a [Tf_2N] anion. Black particles, carbon; red, oxygen; blue, nitrogen; green, fluorine; yellow, sulfur. Hydrogen not shown.

of a liquid surface. In our case, they are used to define the distance of water and ions from the cholesterol/water interface and to measure the volume occupied by the bilayer.

The intrinsic density profile along z referred to the instantaneous position of the upper [$z_U(x, y)$] and lower [$z_L(x, y)$] surface of the bilayer has been computed for the center of mass of the imidazolium ring, the tip of the alkane tail of $[C_4mim]^+$, represented by the butyl C atom furthest from the imidazolium ring, and the center of mass of the anion (either $[Cl]^-$ or $[Tf_2N]^-$). The results are shown in Figure 5.

In the case of both [C_4mim][Cl] and [C_4mim][Tf_2N], nonvanishing density contributions appear for $z_L \leq z \leq z_U$, that is, inside the volume attributed to the bilayer. This confirms that ions are at least partially incorporated into the model membrane, potentially altering properties such as surface tension, bending rigidity, and, more importantly, permeability. The fine details of this incorporation, however, are different for the different cases.

In the case of [C_4mim][Cl], for instance, analysis of the density profiles shows that the most apparent penetration of the cholesterol bilayer is due to the butyl tail of the cation. In the case of [C_4mim][Tf_2N], instead, both the cation and anion display some penetration into the bilayer, but the ion incorporation is apparently more important for the $[Tf_2N]^-$ anion. In other words, the density profiles computed with respect to the intrinsic cholesterol water interface confirm the qualitative results inferred from visual inspection of simulation snapshots.

In all cases, the incorporation of ions from either [C_4mim][Cl] or [C_4mim][Tf_2N] into cholesterol is quantitatively small, corresponding, on average, to ~0.2 ions per square nanometer of bilayer. Nevertheless, the ions' incorporation into the membrane, taking place on the nanosecond time scale of our simulations, is, indeed, remarkable, especially considering that dynamical processes involving cholesterol and IL ions are relatively slow because of the nonnegligible size and high viscosity of all these species. The fast incorporation of ions into the bilayer therefore suggests that the initial stages of IL−cholesterol interaction proceed downhill, unopposed by sizable activation barriers.

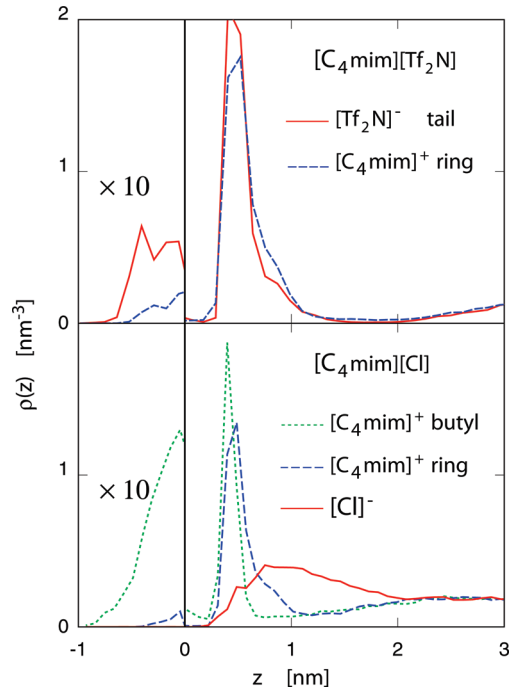

Figure 5. Density profiles along z of [C_4mim][Tf_2N] (upper panel) and [C_4mim][Cl] (lower panel) referred to the intrinsic cholesterol surface (see text) closest to the ion. $z = 0$ marks the position of the intrinsic surface. Data are multiplied by 10 for $z \leq 0$.

Other quantities can be computed, as well. For instance, the bilayer average thickness can be computed from z_U and z_L as follows:

$$\langle \Delta z_{Ch} \rangle = \frac{1}{A} \int [z_U(x, y) - z_L(x, y)] \, dx \, dx \qquad (1)$$

where the integral extends over the area, A, of the simulation box cross section. Then the addition of the electrolyte has a small but still detectable effect on $\langle \Delta z_{Ch} \rangle$. In particular, we find that $\langle \Delta z_{Ch} \rangle = 40.71 \pm 0.02$ Å for the bilayer in contact with pure water. The thickness expands to $\langle \Delta z_{Ch} \rangle = 41.21 \pm 0.02$ Å when the bilayer is in contact with the [C_4mim][Cl] solution and expands even more to $\langle \Delta z_{Ch} \rangle = 41.50 \pm 0.02$ Å in the case of [C_4mim][Tf_2N]. On the other hand, addition of NaCl or LiCl to water has a qualitatively similar but quantitatively much reduced effect, resulting in changes of $\langle \Delta z_{Ch} \rangle$ at the limit of our statistical error bars.

In all cases, the relative variations of $\langle \Delta z_{Ch} \rangle$ are not very big, but the 2% volume expansion observed for [C_4mim][Tf_2N] is still remarkable, and it is likely to be directly related to the partial incorporation of the $[Tf_2N]^-$ anion into the membrane.

Surface tension and bending rigidity can be obtained by analyzing the q-dependence of the equilibrium fluctuations for the geometric surfaces $z_U(x, y)$ and $z_L(x, y)$.[21] Differences with the case of the bilayer in pure water, however, are not statistically significant. The exception is represented by the fluctuations of $\langle \Delta z_{Ch} \rangle$, which can be computed very accurately. The results show that, despite the slight increase in $\langle \Delta z_{Ch} \rangle$, the equilibrium fluctuations of the average $z_U(x, y)$ and $z_L(x, y)$ position decreases systematically in going from pure water to [C_4mim][Cl] and then to [C_4mim][Tf_2N]. Fluctuations in Δz_{Ch}, of course, are easily translated into fluctuations of the volume occupied by cholesterol, which in turn provide an estimate for the isothermal compressibility of the bilayer. The results, that

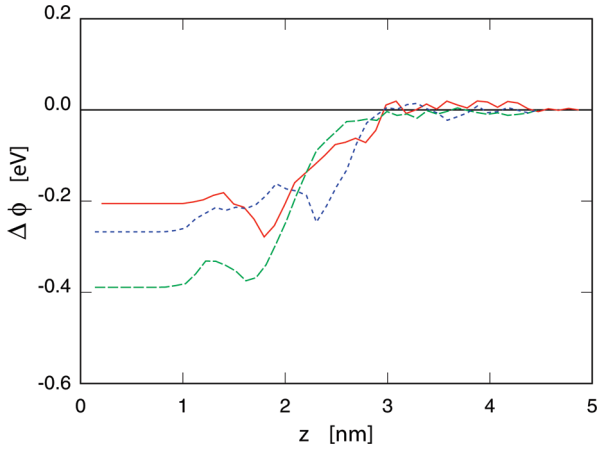

Figure 6. Electrostatic potential along the direction z perpendicular to the cholesterol/water solution interface. Solid line (blue), [C_4mim][Tf_2N]; dashed line (green), [C_4mim][Cl]; dotted line (red), [Na][Cl]. The origin ($z = 0$) corresponds to the center of the cholesterol bilayer. The computed potential includes IL and water contributions and excludes cholesterol contributions.

is, $B_T = 37.8 \pm 0.2$, 41.0 ± 0.2, and 44.8 ± 0.2 kbar for cholesterol in water, [C_4mim][Cl], and [C_4mim][Tf_2N], respectively,[24] point to a sizable effect of IL adsorption on the mechanical properties of the bilayer.

The trajectories accumulated during the simulations have been used to compute the planar average of the charge density, from which the electrostatic potential across the water−cholesterol interface has been computed. To isolate the electrostatic interaction between the water solution and cholesterol, we included the contributions due to the IL and to water, but we excluded the (small) charge density of cholesterol. In all cases, including [Na][Cl] and [Li][Cl], the bilayer is at a negative potential with respect to the bulk solution. The electrostatic double layer is fairly thick, extending ∼1 nm from the water−cholesterol interface (Figure 6). Moreover, the potential drop is smallest for [Na][Cl] ($\Delta\phi = \phi$(solution) − ϕ(bilayer) = 0.20 V), it increases slightly for [C_4mim][Tf_2N] ($\Delta\phi = 0.24$ V), and it is highest for [C_4mim][Cl] ($\Delta\phi = 0.40$ V). The observed trends are easily understood by considering that in the case of [C_4mim][Tf_2N], the thick deposit is locally nearly neutral, and the resulting $\Delta\phi$ is not very different from that of [Na][Cl], whose charge separation is fairly limited. In the case of [C_4mim][Cl], instead, the competition of $[C_4\text{mim}]^+$ adsorption and $[Cl]^-$ solvation enhances the charge separation and the size of the electrostatic double layer.

V. Summary and Conclusions

The most remarkable result of our investigation of an amphiphile bilayer in contact with an IL−water solution is the apparent qualitative agreement of the computational and experimental picture for these systems. Despite differences in the bilayer composition, made of cholesterol instead of phospholipids, and despite the short time span of the simulations, computations do reproduce the strong affinity of IL for organic amphiphile membranes. In the case of [C_4mim][Cl], a compound of high water solubility, we observe a sizable but not complete adsorption at the cholesterol−water interface, coexisting with residual solubility of dissociated $[C_4\text{mim}]^+$ and $[Cl]^-$ ions in water. Adsorption concerns mainly the $[C_4\text{mim}]^+$ cation and is accompanied by limited but still apparent inclusion of the butyl tail into the bilayer.

In the case of [C_4mim][Tf_2N], instead, the hydrophobic salt precipitates out of the water solution, and after a fairly long relaxation time, it gives rise to a thick IL film at the water−cholesterol interface. Residual solubility manifests itself in a few free ions dissolved in water and in molecularly thin loops developing from the IL film and extending into water. In the largest sample we simulated for [C_4mim][Tf_2N], a nanometric IL droplet remains floating in water for more than 10 ns. It is likely, however, that even this residual isolated aggregate would migrate toward the water−organic interface, if only simulations could be continued for much longer times. The bulky and relatively hydrophobic $[Tf_2N]^-$ anion is the electrolyte species most readily incorporated into the cholesterol bilayer. This, in turn, promotes limited penetration of the cation imidazolium ring and significantly reduces the solubility of the butyl chain in cholesterol.

Since cholesterol is a neutral and weakly polar molecule, the close association between the bilayer and either [C_4mim][Cl] or [C_4mim][Tf_2N] has to be driven by dispersion forces and hydrophobic/hydrophilic interactions. This is confirmed also by benchmark computations for [Na][Cl] and [Li][Cl] solutions in contact with the cholesterol bilayer that show very limited mutual interaction between the ions and the organic portion of the system.

Several times in the present paper, we emphasized that diffusion and mixing of fairly complex organic molecules are relatively slow processes whose kinetics might include time scales longer, probably much longer, than the simulation time span. Nevertheless, the qualitative trends discussed above emerge clearly from the simulation results already within the first few nanoseconds of equilibration, lending credibility to the qualitative picture provided by computations. Moreover, the fact that the association and incorporation of IL with cholesterol already take place within a few nanoseconds suggests that these processes are virtually barrierless, at least in their initial stages.

The observation of more drastic rearrangements, such as the removal of lipid molecules or, even more, those leading to poration, are prevented by the short time scale of atomistic simulation and, perhaps, by the small size of the simulated samples. In fact, the macroscopic times measured by experiments imply that these processes are highly activated, and a minimum system size might be required to observe the nucleation of extended defects and pores, in particular.

The encouraging correspondence of computational and experimental results opens the way to a systematic investigation of the interaction mechanisms and the changes in the membrane properties due to the IL solution. This, in turn, might have toxicology applications, and simulations could be used for a preliminary identification of strong, potentially dangerous IL−membrane interactions.

It would be important to extend the investigation of biological effects of ILs, first of all, to phospholipid bilayers and then to other classes of biological structures. Experimental measurements of proteins' activity in IL solutions are available[25,26] and represent an obvious target for computational investigations.

Perhaps more importantly, the characterization and the full understanding of the variation in the membrane structure, dynamical properties, and, in particular, permeability might open the way to biomedical applications, especially in drug delivery. Then the nearly unlimited tunability of chemical physics properties often attributed to IL could provide a decisive advantage for specific developments. In particular, the electrostatic double layer developing at the cholesterol-water interface because of the IL adsorption might provide an additional and tunable parameter for the regulation of processes of biomedical interest.

References and Notes

(1) Welton, T. *Chem. Rev.* **1999**, *99*, 2071–20831999. Seddon, K. R. *J. Chem. Technol. Biotechnol.* **1997**, *68*, 351.

(2) Holbrey, J.; Seddon, K. R. *Clean Products Processes* **1999**, *1*, 223–236. Rogers, R. D.; Seddon, K. R.; Eds. *Ionic Liquids: Industrial Applications for Green Chemistry*; American Physical Society: Washington, DC, 2002, p 818.

(3) See, for instance, Coulin, D. J.; Bernot, R. J.; Docherty, K. M.; Dixon, J.-N. K.; Maginn, E. J. *Green Chem.* **2006**, *8*, 82–90, and references therein.

(4) Evans, K. O. *Colloids Surf., A* **2006**, *274*, 11.

(5) Evans, K. O. *J. Phys. Chem. B* **2008**, *112*, 8558–8562.

(6) Evans, K. O. *Int. J. Mol. Sci.* **2008**, *9*, 498–511.

(7) Limited additional measurements have been performed for $[BF_4]^-$ and $[PF_6]^-$ coupled to $[NH_4]^+$.

(8) Burgess, D. J. In *Encyclopedia of Pharmaceutical Technology*, 2nd ed.; Swarbrick, J., Boylan, J. C., Eds.; Marcel Dekker: New York, 2002. O'Driscoll, C. M.; Griffin, B. T. *Adv. Drug Delivery Rev.* **2007**, *60*, 617–624.

(9) Philippot, J. R.; Milhaud, P. G.; Puyal, C. O.; Wallach, D. F. H. In *Liposomes as Tools in Basic Research and Industry*; Philippot, J. R., Schuber, F. Eds.; CRC Press: Boca Raton, FL, 1995; pp 41−75.

(10) Ambade, A. V.; Savarian, E. N.; Thayumanavan, S. *Mol. Pharm.* **2005**, *2*, 264–272. Basu, S.; Vutukuri, D. R.; Thayumanavan, S. *J. Am. Chem. Soc.* **2005**, *127*, 16794–16795.

(11) Cromie, S. R. T.; Del Pópolo, M. G.; Ballone, P. *J. Phys. Chem. B* **2009**, *113*, 4674–4687.

(12) Cromie, S. R. T.; Del Pópolo, M. G.; Ballone, P. To be published.

(13) Low temperature phase: Shieh, H.-S.; Hoard, L. G.; Nordman, C. E. *Nature* **1977**, *267*, 287–289. Shieh, H.-S.; Hoard, L. G.; Nordman, C. E. *Acta Crystallogr. B* **1981**, *37*, 1538–1543. High temperature phase: Hsu, L.-Y.; Kampf, J. W.; Nordman, C. E. *Acta Crystallogr. B* **2002**, *58*, 260–264.

(14) Craven, B. M. *Nature* **1976**, *260*, 727–729.

(15) Voth, G. A.; Wu, Y.; Tepper, H. L. *J. Chem. Phys.* **2006**, *124*, 024503.

(16) Canongia Lopes, J. N.; Deschamps, J.; Padua, A. A. H. *J. Phys. Chem. B* **2004**, *108*, 2038–2047. Canongia Lopes, J. N.; Padua, A. A. H. *J. Phys. Chem. B* **2004**, *108*, 16893–16898. See also (additions and corrections) Canongia Lopes, J. N.; Deschamps, J.; Padua, A. A. H. *J. Phys. Chem. B* **2004**, *108*, 11250.

(17) It is important to note that the mixing rules for the Lennard-Jones coefficients adopted in ref[16] are $\sigma_{ij} = (\sigma_{ii}\sigma_{jj})^{1/2}$, $\varepsilon_{ij} = (\varepsilon_{ii}\varepsilon_{jj})^{1/2}$, and differ from the most popular Berthelot rules (J. N. Canongia Lopes and A. A. H. Padua, private communication). This point is discussed and clarified in. Canongia Lopes, J. N.; Padua, A. A. H. *J. Phys. Chem. B* **2006**, *110*, 19586–19592.

(18) Tosi, M. P.; Fumi, F. G. *J. Phys. Chem. Solids* **1964**, *25*, 45.

(19) Koneshan, S.; Rasaiah, J. C.; Lynden-Bell, R. M.; Lee, S. H. *J. Phys. Chem. B* **1998**, *102*, 4193–4204.

(20) Smith, W.; Leslie, M.; Forester, T. R.; *DL-POLY, Version 2.14*; Daresbury Laboratories: Daresbury, Warrington, UK, 2003.

(21) Safran, S. A. *Statistical Thermodynamics of Surfaces, Interfaces, and Membranes*; Addison-Wesley: Reading, MA, 1994.

(22) Del Pópolo, M. G.; Mullan, C. L.; Holbrey, J. D.; Hardacre, C.; Ballone, P. *J. Am. Chem. Soc.* **2008**, *130*, 7032–7041.

(23) Chacón, E.; Tarazona, P. *Phys. Rev. Lett.* **2003**, *91*, 166103.

(24) The bulk moduli computed for cholesterol in water and in IL solutions at $T = 280$ K are $\sim$1/2 of the value obtained for the low-temperature crystal phase of cholesterol using the same interatomic potential.

(25) Laszlo, J. A.; Compton, D. L. *J. Mol. Catal. B: Enzym.* **2002**, *18*, 109–120.

(26) Compton, D. L.; Laszlo, J. A. *J. Electroanal. Chem.* **2002**, *520*, 71–78.

JP904060Y